CHAPTER III

ELECTROCHEMICAL INVESTIGATION OF POLYMER FUNCTIONALIZED REDUCED GRAPHENE OXIDE / ZINC OXIDE NANOCOMPOSITES FOR THE DETECTION OF p-AMINOPHENOL

3.1 INTRODUCTION

Aminophenols are well known aromatic compounds that exist in three isomeric forms at which the oxidizable NH_2 and OH groups are positioned around the benzene ring [1-2]. p-Aminophenol, an aromatic compound is an important intermediate formed during the manufacture of analgesic and antipyretic drugs. It is toxic to aquatic life, found in effluent wastes from oil refineries, rubbers, lubricants and textiles It is also widely used in photography and chemical dye industries and is considered as a highly toxic pollutant [3]. The exposure to p-Aminophenol leads to nephrotoxicity and teratogenic effects that is harmful for humans, animals and plants [4]. Several methods have been used for the last few decades for the determination of p-aminophenol. Electrochemical technique has received much attention and has been used widely because of its low cost, simplicity, high selectivity and sensitivity [5-6].

Graphene, a single layer of sp^2 hybridized carbon atoms, packed into a dense honeycomb crystal structure has attracted significant research interest because of its unique structure and extraordinary properties like high conductivity and high surface area [7]. It possesses various material parameters such as superior mechanical stiffness, strength and elasticity, very high electrical and thermal conductivity that has versatile applications in the areas of supercapacitor, transistor, solar cells, batteries, fuel cells, hydrogen storage, nanoelectronics, electrocatalysis, sensors, electrochemical devices and electromechanical resonator [8]. Recently, it has been reported that graphene on making composite with metals, metal oxides, metal organic frameworks, polymers, and carbonaceous materials, it acquires excellent chemical stability that exhibit a remarkable electrochemical biosensing capacity in detecting electro active biomolecules [9]. Chitosan (CS) is a linear b-1,4-linked polysaccharide that possesses distinct chemical and biological properties, because of its reactive amino and hydroxyl groups in its linear high molar mass poly

glucosamine chains which are amenable to chemical modification. It has an excellent characteristic such as film-forming ability, biocompatibility, non-toxicity, good water permeability, high mechanical strength and adhesion [10-12]. Metal nanoparticles incorporated onto the polymer functionalized graphene sheets provide tunable novel properties which can be exploited for different applications. These hybrid nanocomposites can accelerate the charge transfer rate between the electrode and absorbed molecules, leading to rapid generation of electrical response [13]. Among these metal oxides, zinc oxide (ZnO) has attracted much attention due to its unique properties such as optical, electronic, optoelectronic, and biocompatible properties [14]. ZnO is one of the most promising semiconductors that exhibit a hexagonal wurtzite structure with a broad band gap of 3.37 eV and high exciton binding energy of 60 MeV that has been potentially applied in various fields such as catalysis, sensors, photonic detectors, photovoltaics, optoelectronic devices and polarized light emitting devices [15]. Hence in this present work, chitosan functionalized reduced graphene oxide/ zinc oxide nanocomposites are synthesized by chemical reduction method. The synthesized nanocomposites are characterized using FT-IR, XRD, SEM, EDAX, HR-TEM and SAED analysis. The electrochemical sensing of p-Aminophenol is investigated using cyclic voltammetry.

3.2. EXPERIMENTAL PROCEDURE

3.2.1 Reagents

Graphite powder, Conc.sulphuric acid (98% H_2SO_4), potassium permanganate (KMnO4), hydrogen peroxide solution (30% H_2O_2), sodium nitrate ($NaNO_3$), sodium hydroxide (NaOH) and zinc acetate, sodium borohydride ($NaBH_4$), aminophenol are of analytical grade, purchased from sigma Aldrich and are used as received without further purification.

3.2.2 Synthesis of reduced graphene oxide / chitosan / Zinc oxide nanocomposites

The zinc oxide nanoparticles decorated chitosan functionalized reduced graphene oxide nanocomposites are synthesized by chemical reduction method. To prepare rGO/CS/ZnO nanocomposites, the prepared rGO/CS solution is dispersed in 50 ml of distilled water by ultrasonication for 1hour to form the aqueous rGO/CS

solution. About 0.002M of zinc acetate is taken in 50 ml of distilled water and stirred for 1hour at room temperature. Thus the stirred zinc acetate solution is added dropwise into the above dispersed rGO/CS solution under constant stirring. 25 mg of $NaBH_4$ is taken in 50 ml of distilled water and stirred for 1hour separately. The stirred $NaBH_4$ solution is added drop wise into the above mixture. The reaction mixture is stirred for 4 hours at 60°C. The formed solution is left undisturbed for overnight and the resultant supertant is filtered and washed rigorously by centrifuging at 8000 rpm. It is then dried in oven at 60 °C for 4 hours and the sample is grinded finely to form the rGO/CS/ZnO nanocomposites [16-17]. The same procedure is followed to prepare various concentrations of (0.004 M, 0.006 M, 0.008M and 0.01M) zinc oxide naoparticles incorporated rGO/CS nanocomposites.

3.3 RESULTS AND DISCUSSION

3.3.1 FT-IR Spectral Analysis

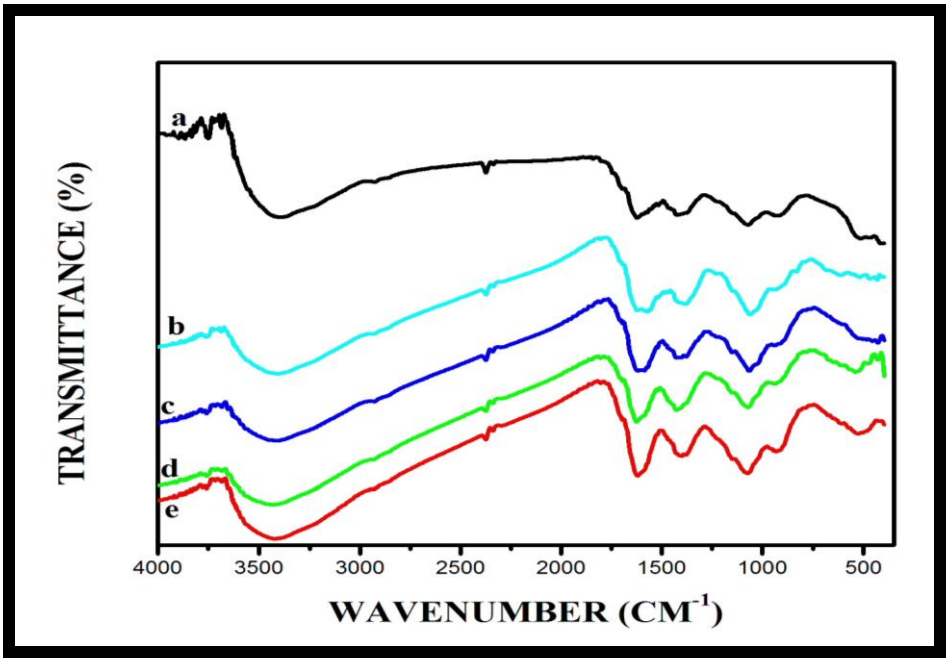

Figure 3.1(a-e) FT-IR Spectral Analysis of various concentrations (a) 0.002 M (b) 0.004 M (c) 0.006 M (d) 0.008 M and (e) 0.01 M of Zinc oxide nanopaticles on the surface of rGO/CS nanocomposites

The bonding interactions between the prepared rGO/CS/ZnO nanocomposites are investigated using FT-IR spectral analysis. Figure 3.1 (a-e) shows the FT-IR Spectral Analysis for different concentrations 0.002 M, 0.004 M, 0.006 M, 0.008 M and 0.01 M of zinc oxide nanoparticles on the surface of rGO/CS nanocomposites. It is observed from the Figure 3.1(a-e) that the band at 3404 cm^{-1} corresponds to the coupling of N-H stretching vibration of amine group of chitosan and O-H stretching vibration of water molecules. The band observed at 1640 cm^{-1} is the characteristic band of -N=N that indicates the existence of chemical interaction between rGO and CS. The bands at 1413 cm^{-1} and 953 cm^{-1} corresponds to C=C stretching vibrations and C-O stretching vibrations respectively. The band observed around 458 cm^{-1} indicates the Zn-O stretching vibration [18-19].

It is observed that on further increasing the concentration of ZnO nanoparticles from 0.002 M to 0.01 M, the characteristic band of O-H gets shifted from 3404 cm^{-1} to 3441 cm^{-1}. The decrease in the intensity of the bands may be due to the formation of hydrogen bond between rGO/CS and ZnO. The band at 1492 cm^{-1} for rGO-CS is shifted to 1484 cm^{-1} because of the decoration of ZnO on the surface of rGO/CS that attributes to the interaction of COO– group of CS with ZnO. It is further evident that the characteristic Zn-O stretching vibration gets shifted to higher wavenumber with increase in the depth of the band [20]. This may be due to its strong interaction with carboxylic functional groups of rGO/CS. These results clearly indicates the successful decoration of ZnO nanoparticles on the surface of rGO/CS nanocomposites

3.3.2 XRD Structural Analysis

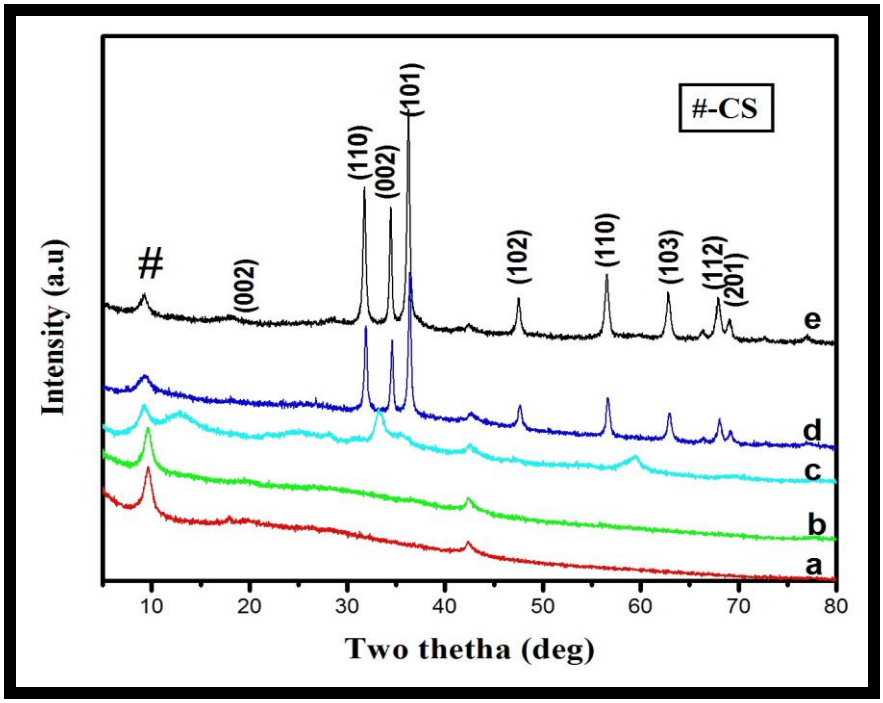

Figure 3.2(a-e) XRD analysis of various concentration (a) 0.002M (b) 0.004M (c) 0.006M (d) 0.008M and (e) 0.01Mof Zinc oxide nanopaticles on the surface of rGO/CS nanocomposites

The X-ray diffraction (XRD) is the most widely used technique to measure the spacing between layers or rows of atoms and to determine the crystallite size of the synthesized nanocomposites. Figure 3.2(a-e) shows the XRD pattern for various concentrations 0.002M, 0.004M, 0.006M, 0.008M and 0.01M of zinc oxide nanoparticles on the surface of rGO/CS nanocomposites. It is observed from Figure 3.2 (a-b) that the peak at 10.9^{o} corresponds to the plane of chitosan. The broad peak at 20.3^{o} corresponds to the (002) plane of reduced graphene oxide and the small additional peak at 42^{o} corresponds to the (001) plane that may be due to the incomplete oxidation of graphite [21]. It is further observed that due to low concentration of zinc acetate, no diffraction peaks of zinc oxide nanoparticles is observed for low concentrations of zinc acetate (0.002M and 0.004M) indicating the strong binding of chitosan into the prepared nanocomposites. It is further evidenced from Figure 3.2 (c-e) that on increasing the concentration of zinc acetate (0.006M,

0.008M and 0.01M) the diffraction peaks centered at 2θ of 31.8 ^{o}, 34.5 ^{o}, 36.2 ^{o}, 47.5 ^{o}, 56.6 ^{o}, 62.8 ^{o}, 67.9 ^{o} and 69.1 ^{o} corresponds to (100) (002) (101) (102) (110) (103)(112) and (201) planes of wurtzite structure of Zinc oxide nanoparticles, which is well matched with the standard JCPDS card no. 36-1451 [22]. It is further observed that by increasing the concentration of zinc acetate, the intensity of diffraction peaks of zinc oxide nanoparticles increases with decrease in intensity of chitosan peaks. The sharpness and the intensity of the peaks indicate the well crystalline nature of the prepared nanocomposites.

The crystallite size is calculated by using Debye Scherrer's formula.

$$D = K\lambda/\beta\cos\theta$$

Where D is the crystalline size (nm), K is a constant equal to 0.9, β is the full width half maximum height of the diffraction peak at an angle θ and λ is wavelength (.λ=1.541Å)

The calculated crystallite size is found to be about 27.3 nm, 33.4 nm and 34.9 nm for 0.006 M, 0.008 M and 0.01 M of ZnO nanoparticles respectively. The crystallite size of zinc oxide nanoparticles increases gradually on increasing the concentration of zinc acetate from 0.006 M to 0.01 M. This may be due to heavy loading of zinc oxide nanoparticles on the surface of rGO/CS nanosheets. These results clearly indicate that ZnO nanoparticles are successfully formed on the surface of rGO/CS nanocomposites.

3.3.3 SEM Analysis

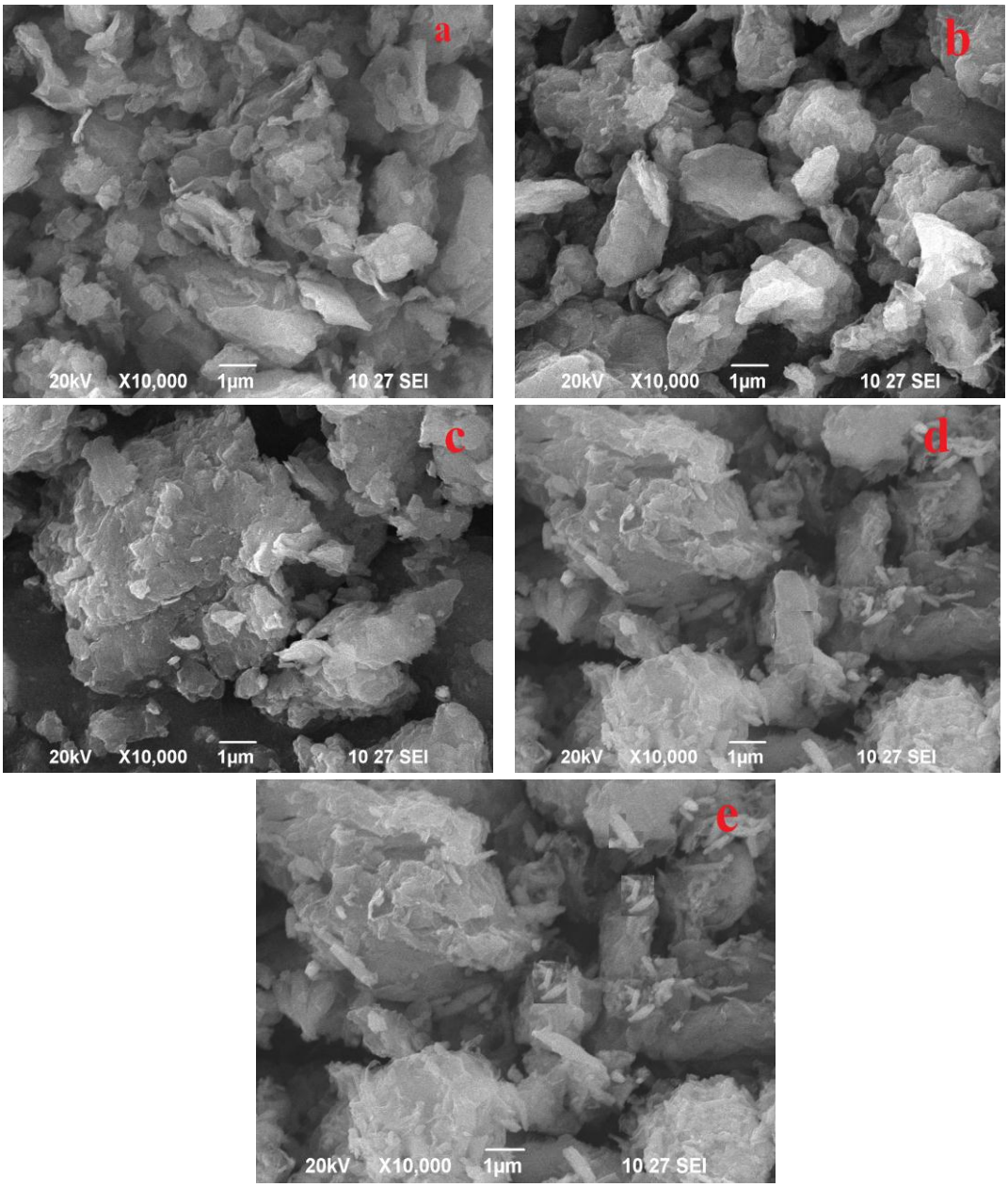

Figure 3.3 (a-e) SEM images for various concentration (a) 0.002M (b) 0.004M (c) 0.006M (d) 0.008M and (e) 0.01M of Zinc oxide nanoparticles incorporated on rGO/CS nanocomposites.

The surface morphology of the synthesized rGO/CS/ZnO nanocomposites is characterized using Scanning Electron Microscopy. Figure 3.3 (a-e) shows the SEM images for various concentrations 0.002 M, 0.004 M, 0.006 M, 0.008 M and 0.01 M of zinc oxide nanoparticles incorporated on rGO/CS nanocomposites [23-24]. It is

observed from the Figure 3.3 (a and b) that the reduced graphene oxide sheets exhibits a typical wrinkled texture with white patches on its surface. The formation of white patches and the roughness of surface indicate that chitosan is well blended onto the reduced graphene sheets. It is also observed that due to low concentration of zinc acetate, there is no obvious formation of ZnO nanoparticles on the surface which implies the strong functionalization of chitosan into the prepared nanocomposites. On further increase in the concentration of zinc acetate from 0.006 M to 0.01 M, the rod shaped zinc oxide nanoparticles are found to be entangled, uniformly distributed and closely anchored onto the surface of rGO/CS nanosheets. Moreover due to the strong functionalization of chitosan, the ZnO nanorods are found to be formed on the surface, edges and in between layers of reduced graphene sheets as depicted in the Figure 3.3 (c- e) which is also evidenced from TEM analysis. Thus on increasing the concnentration of zinc acetate, the number of ZnO nanoparticles on the surface of rGO/CS also increases as evidenced from EDAX analysis. Hence, the SEM micrographs clearly reaveals that ZnO nanoparticles are well incorporated into the chitosan functionalized reduced graphene oxide nanocomposites.

3.3.4. EDAX Analysis

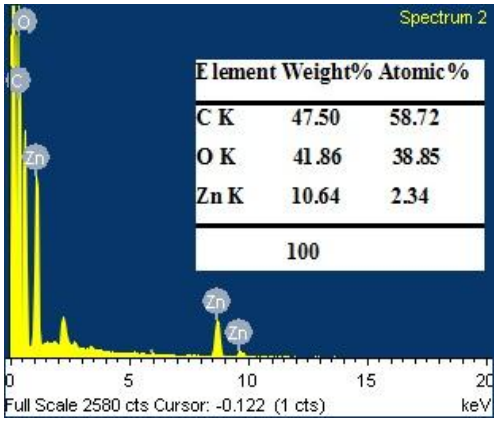

(a)

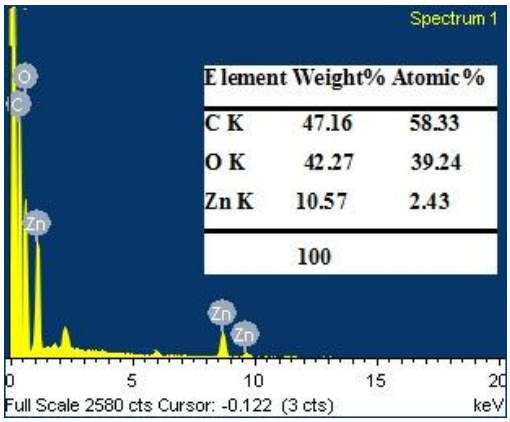

(b)

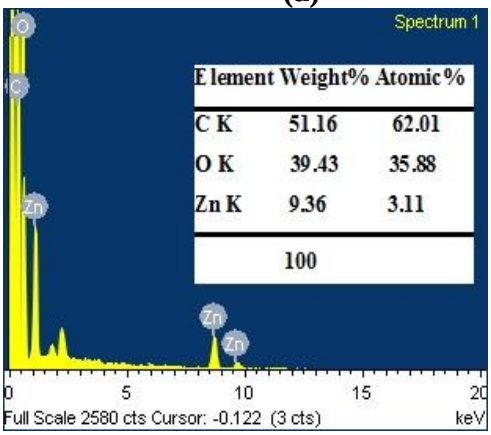

(c)

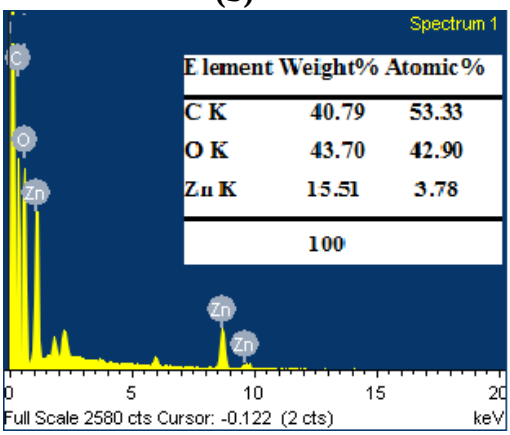

(d)

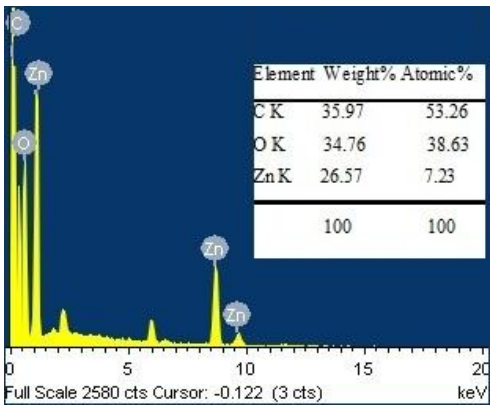

(e)

Figure.3.4.(a-e). EDAX analysis of various concentrations (a) 0.002M (b) 0.004M (c) 0.006M (d)0.008M and (e) 0.01M of zinc oxide nanoparticles incorporated on rGO/CS nanocomposites

The elemental composition of ZnO nanorods decorated chitosan functionalized reduced graphene oxide is studied by energy dispersive analysis of X-rays (EDAX). Figure 3.4 (a-e) depicts the EDAX analysis for various concentration 0.002 M, 0.004 M, 0.006 M, 0.008 M and 0.01 M **o**f Zinc oxide nanorods incorporated on rGO/CS nanocomposites. The elemental presence of carbon, oxygen and zinc without any impurities is confirmed from the Figure 3.4 (a-e) [25-26]. The atomic and weight percentage of carbon, oxygen and zinc for various concentration of zinc oxide nanoparticles are tabulated and shown in the inset of Figure 3.4. It shows that the atomic and weight percentage of Zn increases on increasing the concentration of ZnO which could be evidenced from SEM analysis.

3.3.5 HR-TEM and SAED Analysis

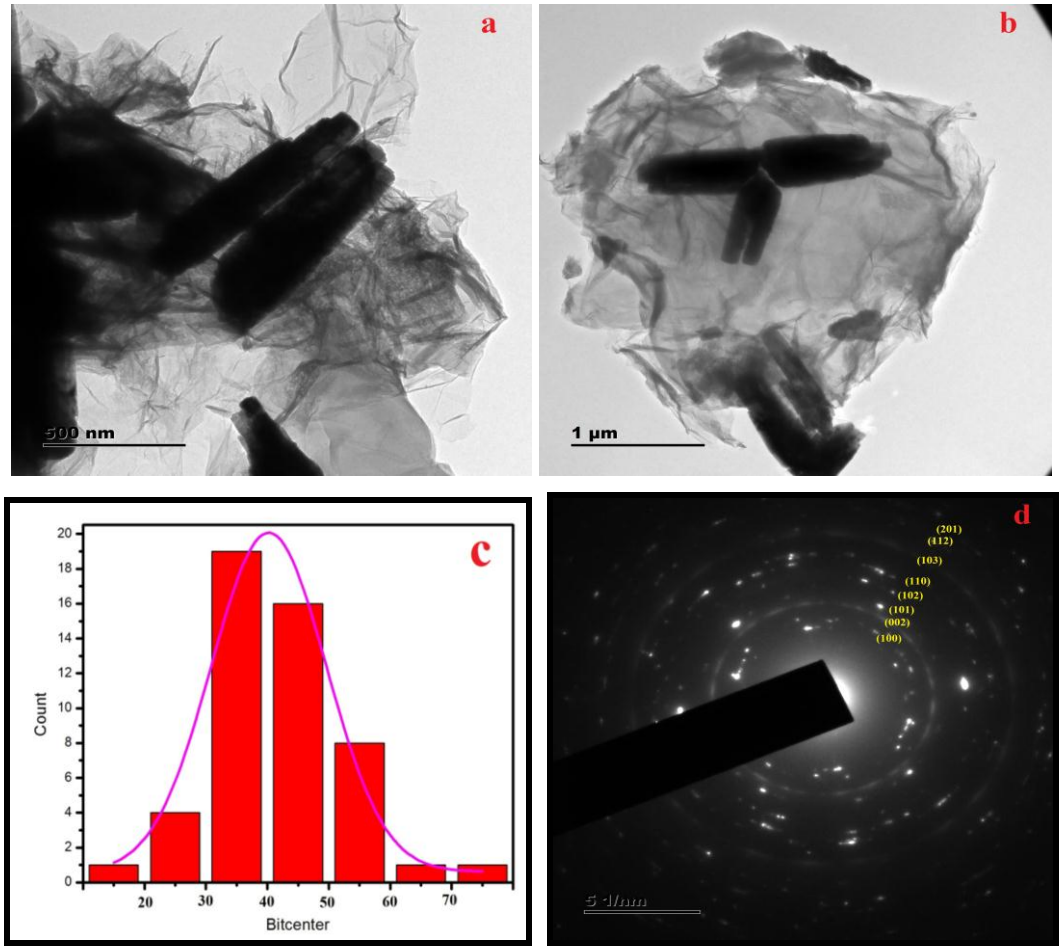

Figure.3.5 (a-b) HR-TEM images with different magnifications (c) Particle size distribution histogram of rGO/CS/ZnO nanocomposites and (d) SAED pattern for 0.008M concentration of Zinc oxide nanoparticles incorporated on rGO/CS nanocomposites

The unique morphology of the prepared nanocomposites is further investigated using HR-TEM analysis. Figure 3.5 (a-b) shows the HR-TEM image and SAED pattern for 0.008M concentration of Zinc oxide nanorods incorporated on rGO/CS nanocomposites. The TEM micrographs depicts that the rod shaped ZnO nanoparticles are uniformly distributed and closely anchored onto the thin crumbled wave like chitosan functionalized reduced graphene oxide nanosheets as depicted in the Figure 3.5 (a-b). The ZnO nanorods are found to be entagled on the surface of rGO/CS nanosheets [27]. Hence, the chitosan matrix helps the ZnO nanorods from aggregation and homogenous dispersion of nanorods on the surface of rGO/CS nanosheets. It is evident that ZnO nanorods are well incorporated onto the surface of rGO/CS nanocomposites, which is beneficial for the electron transfer between the rGO/CS nanocomposites and ZnO nanoparticles. Thus the prepared nanocomposites provide large surface area which helps to reach the active sites for the detection of analytes that improves the sensitivity of the nanocomposites on the surface modified electrode. The average size of about 39 nm is distributed over the surface of rGO/CS as evidenced from Figure 3.5 (c). The SAED pattern for 0.008M concentration of Zinc oxide nanoparticles incorporated on rGO/CS nanocomposites is shown in Figure 3.5(d). The distinct rings with discrete bright spots confirm the polycrystalline nature of the prepared nanocomposites which implies the high degree of crystallization of ZnO nanoparticles with symmetrical orientation [28]. The circular ring pattern corresponds to the lattice planes of (100), (002), (101), (102), (110) and (103) of ZnO nanoparticles which is in good agreement with the XRD results.

3.4. ELECTROCHEMICAL INVESTIGATION OF p-AMINOPHENOL

The prepared rGO/CS/ZnO nancomposites is tested for the electrochemical sensing of p-Aminophenol. Based on the characterization studies 0.008 M of ZnO nanoparticles decorated rGO/CS nanocomposites is chosen to be the electrode material for the electrochemical investigation of p-AP. The electrocatalytic effect of p-AP at 0.008M of rGO/CS/ZnO nanocomposites and various parameters such as the effect of electrolyte and effect of scan rate are also studied.

3.4.1 Electrochemical behavior of modified electrodes

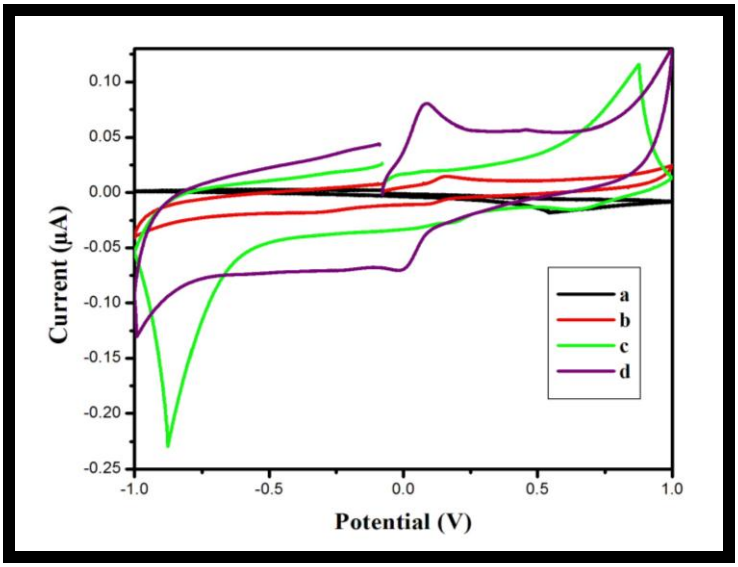

Figure 3.6 (a-d) Cyclic voltagramm curve for (a) GO/GCE (b) rGO/ZnO/GCE (c) rGO/CS/GCE and (d) rGO/CS/ZnO/GCE in the presence of 50µM of p-Aminophenol in 0.1 M Phosphate Buffer Solution (PBS : pH 5) at a scan rate of 20 mV s^{-1}

The electrochemical measurements are performed using electrochemical workstation. Three electrode systems are used containing Glassy Carbon Electrode (3 mm in diameter) as the working electrode, Ag/AgCl (1MKCl) as the reference electrode and platinum wire as the counter electrode. The electrochemical behaviour of p-Aminophenol is investigated in 0.1 M of Phosphate buffer solution (PBS) at pH 5 by cyclic voltammetry (CV) and is recorded in a potential of about -1 to +1 V.

Figure 3.6 (a-d) shows the CV curve for bare GO, rGO/ZnO, rGO/CS and rGO/CS/ZnO modified GCE. It is observed from Figure 3.6 (a), that on addition of 50 µM of p-AP no redox peak is observed for GO indicating that GCE/GO is not activated towards the p-AP sensing [2]. Moreover, a pair of sluggish redox peak current of p-AP is observed at a potential of about E_{pa} = 0.042V and E_{pc} = -0.19V with redox peak current of about Ipa = 0.01µA and Ipc = -0.02 µA for rGO/CS modified GCE as depicted in Figure 3.6 (b). But for rGO/ZnO, a pair of weak redox peak is obtained at a potential of about E_{pa} = 0.16V and E_{pc} = 0.09V with the redox peak current of about I_{pa} = 0.01µA and I_{pc} = -0.01µA. In contrast GCE modified

rGO/CS/ZnO shows a pair of well defined redox peak at a potential about E_{pa}= 0.08 V and E_{pc}= -0.002 V with a redox peak current of about I_{pa} = 0.08 µA and I_{pc} = -0.06 µA. It is clearly observed that the current of rGO/CS/ZnO modified GCE exhibits high redox peak current compared to both rGO/CS and rGO/ZnO. Thus the result reveals that the enhancement of electrocatalytic activity of p-AP at rGO/CS/ZnO is mainly due to the high conductivity, high adsorption, high catalytic ability and the synergetic effect between rGO, CS and ZnO [29-30]. Hence the large surface area of the prepared nanocomposites acts as a active sites for the adsorption of large number of p-AP which helps in the excellent detection of p-AP. Moreover the enhancement of the electrocatalytic activity of the prepared nanocomposites is achieved by optimizing the electrochemical parameters such as pH, scan rate, etc. Hence the proposed sensor can be utilized for the real life detection of p-Aminophenol.

3.4.2 Effect of pH

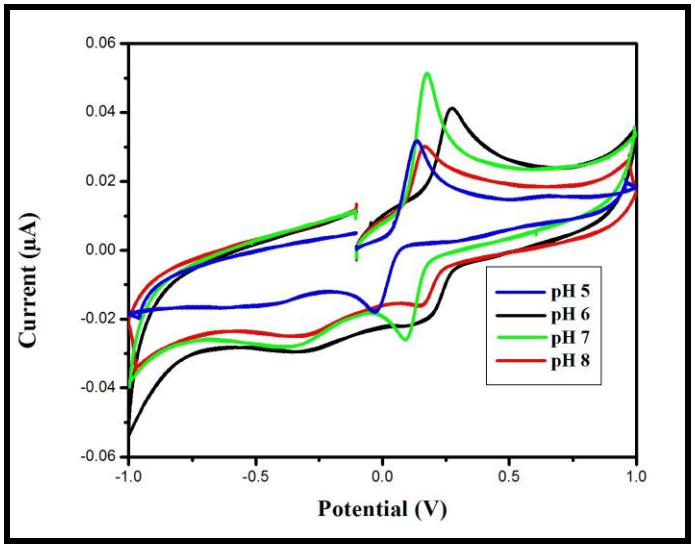

Figure 3.7 (a-b) Effect of pH on the redox peak current of 170 µM of p-AP and its linearity

The electrochemical behaviour of p-AP is strongly dependent on the pH value of the electrolyte solution. The phosphate buffer solution (PBS) with different pH value (pH 5 to pH 8) at the surface of 0.008M rGO/CS/ZnO modified GCE is prepared to investigate the optimum condition for the best electroactivity of p-AP standard solution. Figure 3.7 (a-b) shows the effect of pH on the redox peak current

of 170 µM of p-Aminophenol in 0.1M of PBS with different pH values varying from 5 to 8 at a constant scan rate of 20 mV/s at rGO/CS/ZnO/GCE nanocomposites. The electrochemical response of phenolic compounds is greatly affected by the pH solution, since the electrochemical oxidation and reduction process are directly involved in proton transfer [1, 31]. It is observed from the Figure 3.7 (a) that a pair of well-defined redox peak is obtained for each pH value. It is also observed that on increasing the pH from 5.0 to 7.0 the redox peak currents of p-AP also increases. Thus on further increase in pH 8 both the I_{pa} and I_{pc} get decreases. This reveals that the electrolyte in higher pH of p-AP could not couple well with the rGO/CS/ZnO/GCE, thereby resulting in the lowest redox peak current. The maximum redox peak current is achieved at pH 7.0. Therefore, this phenomenon indicates that 0.1M of phosphate buffer solution (PBS) at pH 7.0 is used for electrochemical investigation of p-AP at rGO/CS/ZnO/GCE due to its sensitive determination of p-AP.

3.4.3 Effect of scan rate

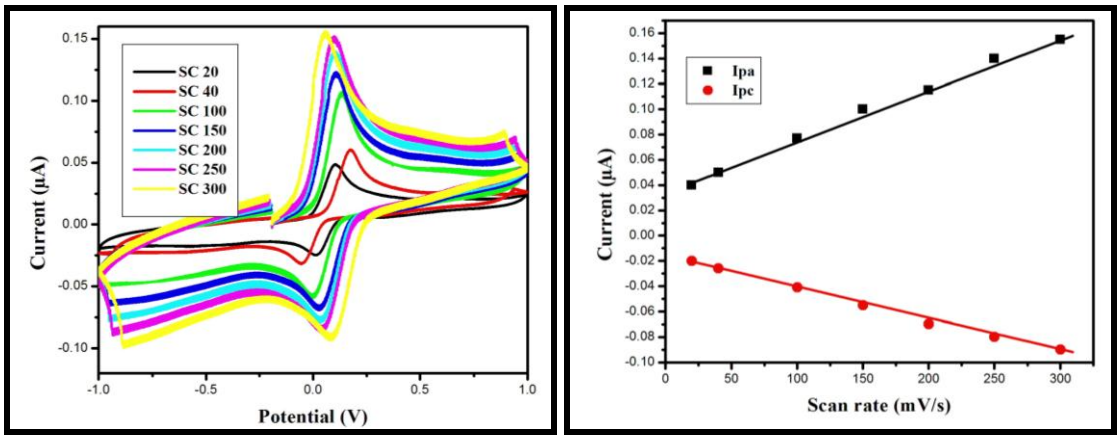

(a) **(b)**

Figure 3.8 (a-b) Effect of scan rate and its linear relationship for 180 µM of p-AP at pH 7 of PBS solution

To investigate the reaction kinetics, the impact of scan rate on the redox peak currents of p-AP at the rGO/CS/ZnO/GCE is investigated by cyclic voltammetry. Figure 3.8 (a-b) shows the cyclic voltagramm curve for effect of scan rate and its linear relationship for 180 µM of p-AP in pH 7 of PBS solution at various scan rates

(20mV/s to 300mV/s). It is clearly observed from the Figure 3.8 (a-b) that the anodic and cathodic peak current increases linearly with the increase in scan rate ranging from 20 mV/s to 300 mV/s, which shows that current is linearly proportional to the scan rate [2-3]. It is observed that as scan rate increases, the anodic peak potential (E_{pa}) is shifted positively and in contrary, the cathodic peak potential (E_{pc}) is shifted negatively. Thus the increased redox peak currents with the increased scan rate from 20 mV/s to 400 mV/s attributes that the redox reaction of p-Aminophenol at the rGO/CS/ZnO/GCE is a diffusion controlled process . The electron transfer is greater at the higher scan rate resulting in the enhanced redox peak current. Hence the scan rate at 20 mV/s is selected as an optimized scan rate for further electrochemical inestigation of p-AP at rGO/CS/ZnO/GCE.

3.4.4 Effect of analyte concentration

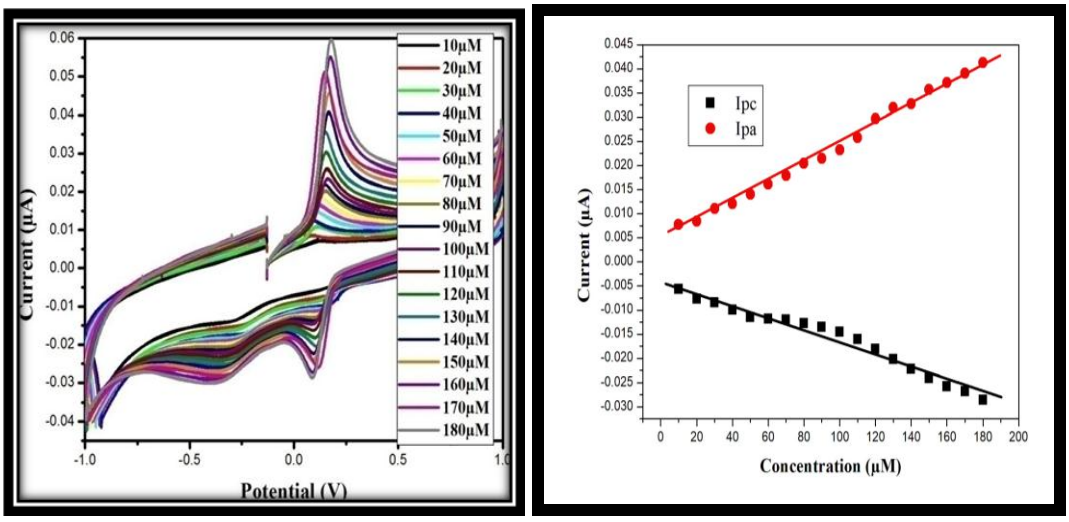

(a) **(b)**

Figure 3.9 (a-b) Cyclic voltagramm curves for 0.008M of rGO/CS/ZnO/GCE towards the detection of various concentrations of p-AP in pH 7of PBS solution at 20mV/s scan rate

The electrochemical responses of p-AP on 0.008M of rGO/CS/ZnO modified GCE at pH 7 of 0.1 M of PBS solution at a scan rate of 20 mV/s is investigated by cyclic voltammetry. Figure 3.9 (a-b) shows the cyclic voltagramm curves for 0.008M of rGO/CS/ZnO/GCE towards the detection of various concentrations of p-AP at pH 7 of PBS solution. It is observed from the Figure 3.9 (a-b) that on

increasing the concentration of p-AP the redox peak current of p-AP also increases linearly [4, 32]. The linearity range observed for 10 µM to180 µM. Thus the enhanced electrochemical activity is due to the large surface area and high electrocatalytic activity of the prepared nanocomposites. These results reveal that the prepared nanocomposites is effective to promote the electron transfer of p-AP which shows good electrocatalytic activity towards the detection of p-AP.

3.5 CONCLUSION

The rGO/CS/ZnO nanocomposites are successfully synthesized by chemical precipitation method and the nanocomposites are characterized using XRD, FTIR, SEM, EDAX, TEM and SAED analysis and further applied for the electrochemical detection of p-AP. The band formed around 458 cm^{-1} indicates the Zn-O stretching vibration. XRD reveals that the intensity of diffraction peaks of zinc oxide nanoparticles increases with decrease in intensity of chitosan peaks. The crystallite size is found to be about 27.3 nm, 33.4 nm and 34.9 nm for 0.006 M, 0.008 M and 0.01 M of ZnO nanoparticles. It is observed from SEM and TEM analysis that the rod shaped ZnO nanoparticles found to be well dispersed onto the polymer functionalized rGO sheets. EDAX analysis reveals the presence of carbon, oxygen and zinc without any impurities that further confirms the formation of rGO/CS/ZnO nanocomposites. The electrochemical behaviour of rGO/CS/ZnO nanocomposite towards the detection of p-AP at the modified glassy carbon electrode is studied. The prepared 0.008M of rGO/CS/ZnO nanocomposites has shown prominent electrochemical behaviour towards the detection of p-AP. The maximum redox peak current is observed for pH 7 of 0.008M of rGO/CS/ZnO nanocomposite is 0.06µA and the wide linear range of about 10µM to 180µM. The nanocomposites show excellent electrocatalytic activity towards the detection of p-AP with a wide linear range from 10 µM to 180 µM. Thus the as prepared nanocomposites hold enormous ability to detect p-Aminophenol in the environment.

REFERENCES

1. J.Vinoth Kumar, R.Karthik, Shen-Ming Chen, K.Saravanakumar, GovindasamyMani, and V.Muthuraj, RSC Advances, DOI: 10.1039/ C6RA03343A, (2016).

2. Junjuan Qian, Depeng Zhang, Lirong Liu, Yinhui Yi., Mwenze Nkulu Fiston, Odoom Jibrael Kingsford and Gangbing Zhu, Journal of The Electrochemical Society. 165 (11) B491-B497, (2018).

3. Graziella Scandurra, Arena Antonella, Carmine Ciofi, Gaetano Saitta and Maurizio Lanza, Sensors, doi:10.3390/s140508926, (2014).

4. Priya Arulselvi Ramasubramanian, Sakthivel Thangavel, Gouthami Nallamuthu., Kiranpreethi Kirabakaran, Vinesh Vasudevan, Kennedy Ravichandran and Gunasekaran Venugopal, Journal of Materials Science: Materials in Electronics. https://doi.org/10.1007/s10854-018-8539-9, (2017).

5. Chethan M kuskur, Kumara Swamy and Jayadevappa, J Anal Bioanal Tech. doi:10.4172/2155-9872.1000260, (2015).

6. Huanshun Yina, Qiang Maa, Yunlei Zhoua, Shiyun Aia and Lusheng Zhu, Electrochimica Acta. 55, 7102–7108, (2010).

7. Chao Xu., Xin Wang and Junwu Zhu, J. Phys. Chem. C**.** 112. 19841–19845, (2008).

8. Huang Lin-jun, Wang Yan-xin, Tang Jian-guo, Wang Hui-min, Wang Hai-bin, Qiu Jian-xiu, Wang Yao, Liu Ji-xian and Liu Jing-quan, Int. J. Electrochem. Sci. 7.11068 – 11075, (2012).

9. Hongqian Bao, Yongzheng Pan, Yuan Ping, Nanda Gopal Sahoo, Tongfei Wu, Lin Li, Jun Li and Leong Huat Gan , Small micro nano, DOI: 10.1002/smll.201100191, (2011)

10. Jiang Yang, Ji-HyukYu, J.Rudi Strickler, Woo-JinChang and Sundaram Gunasekaran., Biosensors and Bioelectronics, 47.530–538, (2013).

11. Zhimin Luo, Dongliang Yang, Guangqin Qi, Lihui Yuwen, Yuqian Zhang, Lixing Weng, Lianhui Wang and Wei Huang, ACS Appl. Mater. Interfaces. 7, 8539−8544, (2015).

12. Richard Justin and Biqiong Cheng, J. Mater. Chem. B, DOI: 10.1039/c4tb00390j, (2014).

13. Mingming Wan, Zhiming Liu, Shaoxin Li, Biwen Yang, Wen Zhang, Xiaochu Qin and Zhouyi Guo, Society for Applied Spectroscopy, DOI:10.1366/12-06777, (2013).

14. Murugan Saranya, Rajendran Ramachandran and Fei Wang, Journal of Science: Advanced Materials and Devices. DOI: 10.1016/j.jsamd. 2016.10.00, (2016).

15. S. Gayathri, P. Jayabal, M. Kottaisamy and V. Ramakrishnan, Journal of Applied Physics. DOI: 10.1063/1.4874877, (2014).

16. Deepak Balram, Kuang-Yow Lian, Neethu Sebastian, A Novel Electrochemical Sensor Based on Flower Shaped Zinc Oxide Nanoparticles for the Efficient Detection of Dopamine, Int.J.Electrochem. Sci., 13, 1542 – 1555, doi:10.20964/2018.02.06, (2018).

17. D Junwei, Z Shiying, Z Tao, S Wei, Gang Wei and Su Zhiqiang, Hydrothermal synthesis of zinc oxide-reduced graphene oxide nanocomposites for an electrochemical hydrazine sensor, RSC Adv, 5, 22935-22942. DOI: 10.1039/c5ra00884k, (2015).

18. Li-Hua Li, Jian-Cheng Deng , Hui-Ren Deng, Zi-Ling Liu and Ling Xin, Synthesis and characterization of chitosan/ZnO nanoparticle composite membranes, Carbohydrate Research, vol.no 345, pg.no : 994–998, (2010).

19. S Anandhavelu, V Dhanasekaran, Hui Joon Park and Hyun-Seok Kim, One-Pot Facile Methodology to Synthesize Chitosan-ZnO-Graphene Oxide Hybrid Composites for Better Dye Adsorption and Antibacterial Activity, Nanomaterials, Vol.7, issue.363, doi:10.3390/nano7110363, (2017).

20. Murugan Saranya, Rajendran Ramachandran, Fei Wang, Graphene-zinc oxide (G-ZnO) nanocomposite for electrochemical supercapacitor applications, Journal of Science: Advanced Materials and Devices. 1 454-460, (2016).

21. Murugan Keerthi, Gopal Boopathy, Shen-Ming Chen, Tse-Wei Chen, Syang-Peng Rwei and Xiaoheng Liu, An Efficient Electrochemical Sensor Based on Ag Nanoparticle Decorated MnO_2/reduced Graphene Oxide Ternary Nanocomposite for Detection of Acetaminophen in Human Urine Sample. Int. J. Electrochem. Sci., doi: 10.20964/2019.01.59, (2019).

22. Linlin Zhong and Kyusik Yun, Graphene oxide-modified ZnO particles: synthesis, characterization, and antibacterial properties, International Journal of Nanomedicine, http://dx.doi.org/10.2147/IJN.S88319.

23. Mukesh Lavkush Bhaisare, Bo-Sgum Wu, Mon-Chun Wu, M. Shahnawaz Khan, Mei-Hwei Tsengb and Hui-Fen Wu, MALDI MS analysis, disk diffusion and optical density measurements for the antimicrobial effect of zinc oxide nanorods integrated in graphene oxide nanostructures, Biomaterials Science DOI: 10.1039/c5bm00342c.

24. Elena Zanni, Chandrakanth Reddy Chandraiahgari, Giovanni De Bellis, Maria Rita Montereali, Giovanna Armiento, Paolo Ballirano, Antonella Polimeni, Maria Sabrina Sarto and Daniela Uccelletti, Zinc Oxide Nanorods-Decorated Graphene Nanoplatelets: A Promising Antimicrobial Agent against the Cariogenic Bacterium Streptococcus mutans, Nanomaterials, doi:10.3390/nano6100179, (2016).

25. S. Gayathri., P. Jayabal., M. Kottaisamy and V. Ramakrishnan. Synthesis of ZnO decorated graphene nanocomposite for enhanced photocatalytic properties. Journal of Applied Physics, DOI: 10.1063/1.4874877, (2014).

26. Fozia Shaheen, Muhammad Hammad Aziz, Mahvish Fatima, Muhammad Ajmal Khan, Faisal Ahmed, Riaz Ahmad, Muhammad Ashfaq Ahmad, Turki S. Alkhuraiji, Muhammad Waseem Akram, Rizwan Raza and Syed Mansoor

Ali, In Vitro Cytotoxicity and Morphological Assessments of GO-ZnO against the MCF-7 Cells: Determination of Singlet Oxygen by Chemical Trapping, Nanomaterials, 8, 539; doi:10.3390/nano8070539, (2018).

27. Yu Zhao, Wenbo Li, Lijia Pan, DongyuanZhai, YuWang, Lanlan Li, WenCheng, WeiYin, XinranWang, Jian-BinXu and Yi Shi, ZnO-nanorods/graphene heterostructure: a direct electron transfer glucose biosensor, Scientific Reports, 6:32327, DOI: 10.1038/srep32327, (2016).

28. Synthesis Characterization, Antimicrobial, Antioxidant, and Cytotoxic Activities of ZnO Nanorods on Reduced Graphene Oxide R. Rajeswari1 · H. Gurumallesh Prabu, J Inorg Organomet Polym, 28 (3), 679-693 (2017).

29. Wei Liu, Preparation of a Zinc Oxide-Reduced Graphene Oxide Nanocomposite for the Determination of Cadmium(II), Lead(II), Copper(II), and Mercury(II) in Water, Int. J. Electrochem. Sci., 12, 5392 – 5403, doi: 10.20964/2017.06.06, (2017).

30. Kh. Ghanbari and S. Bonyadi, An electrochemical sensor based on reduced graphene oxide decorated with polypyrrole nanofibers and zinc oxide–copper oxide p–n junction heterostructures for the simultaneous voltammetric determination of ascorbic acid, dopamine, paracetamol and tryptophan, New Journal of Chemistry, 42(11), 8512–8523.doi:10.1039/c8nj00857d, (2018).

31. A.T.Ezhil Vilian, Vediyappan Veeramani, Shen-Ming Chen, Rajesh Madhu,a Yun, Suk Huh, Young-Kyu Han, Preparation of a reduced graphene oxide/poly-lglutathione nanocomposite for electrochemical detection of 4-aminophenol in orange juice samples, Analytical methods, 00, 1-3, (2013).

32. Huijuan Wang, Siyu Zhang, Shufang Li, and Jianying Qu, Electrochemical sensor based on palladium-reduced graphene oxide modified with gold nanoparticles for simultaneous determination of acetaminophen and 4-aminophenol, (2017).